INVITED PAPER *Special Section on Recent Advances in Ultra-high-speed Photonic Devices for Next-generation Optical Fiber Communications*

High-Speed Frequency Modulated DBR Lasers for Long-Reach Transmission

Takaaki KAKITSUKA[†a)] ***and*** **Shinji MATSUO**[†]**,** ***Members***

SUMMARY We present a novel high-speed transmitter consisting of a frequency modulated DBR laser and optical filters. The refractive index modulation in the phase control region of the DBR laser allows high-speed frequency modulation. The generated frequency modulated signal is converted to an intensity modulated signal using the edge of the optical filter pass band. We present theoretical simulations of high-speed modulation characteristics and extension of transmission reach. With the proposed transmitter, we review the experimental demonstration of 180-km transmission of a 10-Gb/s signal with a tuning range of 27 nm and 60-km transmission of a 20-Gb/s signal.

key words: *DBR laser, frequency modulation, FM/AM conversion, optical filter*

1. Introduction

The explosive growth of network traffic requires large capacity transmission systems. Wavelength division multiplexing (WDM) has been widely used to increase the transmission capacity. Today, wavelength routing technologies provide various functions to realize flexible photonic network. Photonic networks which employ reconfigurable optical add drop multiplexer (ROADM) and optical cross connect (OXC) systems require longer transmission reach compared to conventional networks which employ SDH/SONET systems, since a signal is transmitted through the node without O/E and E/O conversion. Multilevel phase modulation and orthogonal frequency division multiplexing (OFDM) using Lithium Niobate ($LiNbO_3$) modulators have been investigated to enable high-speed and long-reach transmission. However, since the system configuration and operation scheme are complex, application is limited to use in the core network because low cost is essential for the metro and access areas. Therefore, high-speed optical transmitters with simple configuration and operation are required for these areas. Semiconductor-based transmitters are attractive because of their compact size, low power, and high-speed operation. There are two types of transmitters; one employs the direct modulation of single-mode lasers such as distributed feedback (DFB) lasers, distributed Bragg-reflector (DBR) lasers, and vertical cavity surface-emitting lasers (VCSEL), and the other employs external modulation such as electro-absorption modulator integrated DFB (EA-DFB) lasers and Mach-Zehnder interferometer modulators (MZM). Although high-speed operation of up to 40 Gb/s has been reported for directly modulated lasers [1]–[3] and EA-DFB lasers [4], each has the drawback of frequency chirping, which results in degradation of the transmission characteristics with non-dispersion shifted fiber. In addition, the transmission distance rapidly decreases as the bit rate increases. Meanwhile the MZM has achieved both high-speed modulation and chirp reduction, with 200-km transmission demonstrated using the duo-binary modulation format [5]. However, in terms of operational simplicity and cost, on-off keying (OOK) modulation without an external modulator is still advantageous. The high-speed access and metro networks require a cost-effective, long-reach transmission technique without the need for optical and/or electrical dispersion compensation.

Various techniques have been developed to extend the transmission reach of directly modulated lasers [6]–[8]. Direct modulation causes large frequency chirping, which degrades the transmission characteristics. One type is the extra transient chirping caused by relaxation oscillation, and the other is the adiabatic chirping caused by carrier variation in the active region. Recently, the use of optical filtering has been proposed for controlling the frequency chirping [6]–[8]. With this approach, the frequency chirping is suppressed by reducing the intensity modulation index. An optical filter with a narrow pass-band is then employed to enhance the output signal extinction ratio. In addition, optical filtering makes it possible to eliminate the extra transient chirp, thus expanding the transmission reach of a 10-Gb/s signal to 38.5 km [6]. In addition, a novel scheme has been developed that uses the edge of the optical filter pass-band (FM/AM conversion) [7], [8]. With this approach, minimum shift keying (MSK) modulation conditions are applied, whereby the frequency modulation width Δf is half of the bit rate B ($\Delta f = B/2$) [7], [9], [10]. In addition to the enhancement of the extinction ratio, the frequency profile is reshaped by FM/AM conversion as a result of optimizing the filtering function of the optical filter. A 10-Gb/s non-return-to-zero (NRZ) signal has been transmitted over 250 km without optical and/or electrical dispersion compensation [8]. However, the use of direct modulation with MSK modulation is disadvantageous as the bit rate increases. With direct modulation, the frequency modulation width is proportional to the intensity modulation depth. Therefore, to satisfy the MSK condition at a high bit rate, a large modulation depth is needed, which would distort the signals as a result of increased relaxation oscillation.

Manuscript received November 14, 2008.
Manuscript revised February 13, 2009.

[†]The authors are with NTT Photonics Laboratories, NTT Corporation, Atsugi-shi, 243-0198 Japan.
a) E-mail: kaki@aecl.ntt.co.jp

DOI: 10.1587/transele.E92.C.929

Previously, we have proposed a high-speed frequency modulated DBR laser for long-reach transmission [11], [12]. Refractive index modulation of the phase control region with a reverse bias voltage makes it possible to achieve high-speed frequency modulation [13]. The frequency modulated signal is converted to an intensity modulated signal by optical filtering. In addition to extending the transmission reach with a simple transmitter, this scheme has the following advantages: (1) high-speed modulation capability independent of relaxation oscillation frequency, (2) a low modulation voltage due to efficient frequency modulation, (3) wide wavelength tunability via current injection into the DBR region, and (4) high-power operation without signal distortion realized by integrating a semiconductor optical amplifier (SOA) (no pattern effects since the signal is generated without intensity modulation). We have reported the 180-km error-free transmission of a 10-Gb/s signal using super-structure-grating (SSG)-DBR lasers with a wavelength tuning range of 27 nm [11], and the 40-km transmission of a 25-Gb/s signal using a monolithically integrated 4-channel DBR laser array [12].

In this work, we present a theoretical description of the modulation of the frequency-modulated DBR lasers, and its transmission characteristics using optical filters. To demonstrate our approach, we describe 10- and 20-Gb/s operation using frequency modulated SSG-DBR lasers and compare simulations with experiments.

2. Operating Principle

Figure 1 shows the configuration of our proposed transmitter, which consists of a frequency-modulated DBR laser and an optical filter. A DBR laser generates a frequency modulated signal by refractive index modulation of the phase control region. An optical filter is used to convert the frequency modulated signal to an intensity modulated signal by using the edge of the optical filter pass-band. In addition to the FM/AM conversion, control of the frequency chirping makes it possible to realize long-reach transmission. It is assumed the generated intensity modulated signal is transmitted through non-dispersion shifted fiber. In this section, the operating principle of the DBR laser and FM/AM conversion are described theoretically.

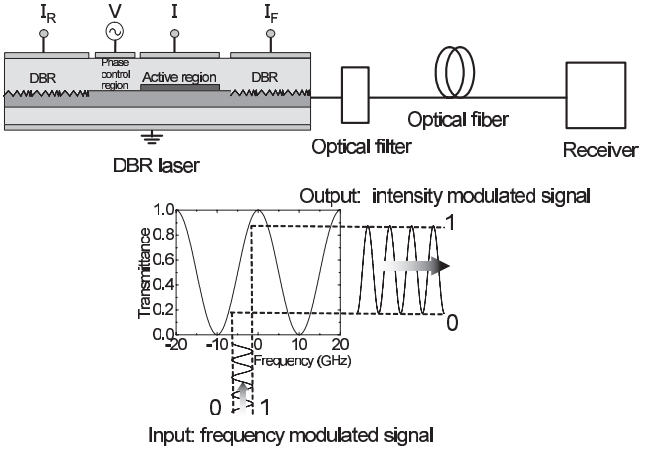

Fig. 1 Schematic of transmitter configuration.

2.1 Frequency Modulation of DBR Laser

As shown in Fig. 1, the DBR laser consists of a DBR region, an active region, and a phase control region. A reverse bias and modulation voltage are applied to the phase control region. The reverse bias modulation induces a refractive index change in the phase control region, which changes the longitudinal lasing mode of the DBR laser. A small signal analysis is useful for understanding the modulation characteristics [14]. The set of rate equations is given by

$$\frac{dN}{dt} = \frac{I}{eV_a} - GS - \frac{N}{\tau_s} \tag{1}$$

$$\frac{dS}{dt} = GS - \frac{S}{\tau_p} + R_{sp} \tag{2}$$

$$\frac{df_0}{dt} = -\frac{f_0}{L}\left(\frac{L_a}{n_{eqa}}\frac{dn_{eqa}}{dN}\frac{dN}{dt} + \frac{L_p}{n_{eqp}}\frac{dn_{eqp}}{dV}\frac{dV}{dt}\right) \tag{3}$$

$$= -\frac{\xi_t c}{4\pi n_{eq}}\left(-\frac{L_a}{L}\alpha_{LEF}g'\frac{dN}{dt} + \frac{L_p}{L}\beta_c\frac{d\alpha_p}{dV}\frac{dV}{dt}\right) \tag{4}$$

where N is the carrier density, S the photon density, f_0 the lasing frequency, V_a the active layer volume, I the injection current in the active region, G the optical gain, g' the differential gain, τ_s the carrier lifetime, R_{sp} the spontaneous emission rate, $n_{eqa(p)}$ the effective index in the active (phase control) region, V the bias voltage in the phase control region, ξ_t the transverse optical confinement, α_{LEF} the linewidth enhancement factor in the active region, β_c the chirp parameter in the phase control region, L the total cavity length, L_a the active region length, and L_p the phase control region length. The effective index $n_{eqa(p)}$ is assumed to be uniform throughout the cavity region. τ_p is the photon lifetime given by

$$\tau_p = \frac{n_{eq}L}{c\left(\xi_t\alpha_a L_a + \xi_t\alpha_p(V)L_p + \frac{1}{2}\ln\left(\frac{1}{R_1R_2}\right)\right)}, \tag{5}$$

where α_a is the propagation loss in the active region, α_p the propagation loss in the phase control region, and $R_{1(2)}$ the reflectivity of the front (rear) DBR region. ξ_t is assumed to be uniform throughout the cavity. α_p depends on the operation bias voltage V.

The frequency response is obtained from Eqs. (1)–(3) as the perturbation of the bias voltage $\Delta V = \Delta V_m e^{2\pi i f t}$, where f is the modulation frequency. The modulation width of the lasing frequency induced by the change in the bias voltage is given by

$$\Delta f_0(f) = -\frac{f_0 L_p}{n_{eq}L}\frac{\partial n_{eq}}{\partial V}\frac{f^2 - f_r^2 - \frac{\Gamma_f}{(2\pi)^2} - if\frac{\Gamma}{2\pi}}{f^2 - f_r^2 - if\frac{\Gamma}{(2\pi)}}\Delta V \tag{6}$$

where

$$f_r = \frac{1}{2\pi}\sqrt{\Gamma_N\Gamma_P + \Gamma_{NP}\Gamma_{PN}} \tag{7}$$

is the relaxation oscillation frequency, and

$$\Gamma = \Gamma_N + \Gamma_P \tag{8}$$

is the decay rate of the relaxation oscillations. The explicit expressions for the parameters are

$$\Gamma_P = \frac{R_{sp}}{S_0} - \frac{\partial G}{\partial S}S_0 \tag{9}$$

$$\Gamma_N = \frac{\partial G}{\partial N}S_0 + \frac{\partial}{\partial N}\left(\frac{1}{\tau_s}\right)N_0 + \frac{1}{\tau_s} \tag{10}$$

$$\Gamma_{PN} = \frac{\partial G}{\partial N}S_0 + \frac{\partial R_{sp}}{\partial N} \tag{11}$$

$$\Gamma_{NP} = G + \frac{\partial G}{\partial S}S_0 \tag{12}$$

$$\Gamma_f = \xi_t \frac{c}{n_{eq}}\frac{\partial \alpha_p}{\partial V}\frac{L_a}{L}\frac{\dfrac{\partial n_{eqa}}{\partial N}}{\dfrac{\partial n_{eqp}}{\partial V}}\Gamma_{NP}S_0 \tag{13}$$

$$= -\frac{L_a}{L}\frac{c\xi_t}{n_{eq}}\frac{\alpha_{LEF}g'}{\beta_c}\Gamma_{NP}S_0, \tag{14}$$

where S_0 is the photon density in the cavity under a static operating condition.

Γ_f is a parameter relating the frequency change in the active region to that in the phase control region. Under a static operating condition, Eq. (6) becomes

$$\Delta f_0(0) = -\frac{f_0 L_p}{n_{eq}L}\frac{\partial n_{eqp}}{\partial V}\left(1 + \frac{\Gamma_f}{(2\pi)^2 f_r^2}\right)\Delta V \tag{15}$$

The first term shows the frequency change caused by the refractive index change in the phase control region, and the second term shows the frequency change caused by the change of carrier density in the active region due to changing the optical loss in the phase control region. Since the frequency modulation width is determined by the L_p/L ratio, not the phase control region length, a large frequency modulation can be obtained with a compact cavity. Therefore, design of the cavity is important to obtain the desired frequency modulation width. Figure 2 shows the dependence of the required L_p/L ratio on the bit rate under MSK frequency modulation conditions ($\Delta f_0 = B/2$). In this calculation, $f_r = 10$ GHz and $\Delta n_{eq}/n_{eq} = 2.4 \times 10^{-4}$. The required L_p/L ratio depends strongly on Γ_f. In a general material for the active region, the linewidth enhancement factor $\alpha_{LEF} = -4\pi f_0(\partial n_a/\partial N)/(cg') > 0$. Therefore, if the chirp parameter for the phase control region $\beta_c = 4\pi f_0(\partial n_p/\partial V)/c(\partial\alpha_p/\partial V) > 0$, $\Gamma_f < 0$. Under this condition, the first and second terms in Eq. (15) cancel each other out and the modulation efficiency decreases. Therefore, the required L_p/L ratio for transmission increases as shown in Fig. 2. To maximize the frequency modulation width, it is essential to suppress Γ_f. As shown in Eq. (13), if the change in the optical loss in the phase control region $\partial\alpha_p/\partial V$ is zero, $\Gamma_f = 0$. In this condition, the output power is constant since the threshold gain does not change during the modulation.

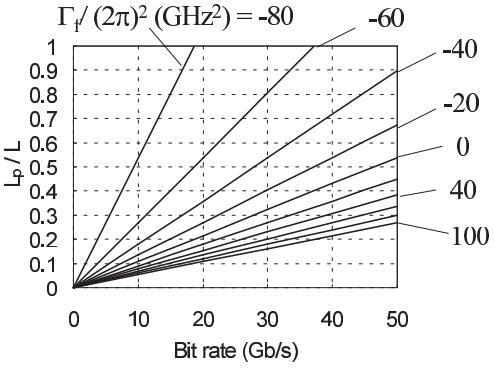

Fig. 2 Relationship between required L_p/L and bit rate under MSK conditions. The parameter $\Gamma_f/(2\pi)^2$ ranges from −80 to 100 GHz^2 in 20 GHz^2 step.

On the other hand, if $\Gamma_f > 0$, since the frequency modulation width increases, the required L_p/L ratio becomes small as Γ_f increases. However, a large Γ_f degrades the modulation characteristics as follows.

Since the intensity modulation is generated by the FM/AM conversion, if the amplitude change is assumed to be proportional to the frequency modulation width, the modulation frequency response is given by

$$\frac{M(f)}{M(0)} = \left|\frac{\Delta f_0(f)}{\Delta f_0(0)}\right| = \frac{f_r^2}{f_r^2 + \dfrac{\Gamma_f}{(2\pi)^2}}\frac{\sqrt{\left(f^2 - f_r^2 - \dfrac{\Gamma_f}{(2\pi)^2}\right)^2 + f^2\left(\dfrac{\Gamma}{2\pi}\right)^2}}{\sqrt{(f^2 - f_r^2)^2 + f^2\left(\dfrac{\Gamma}{2\pi}\right)^2}}. \tag{16}$$

Figure 3 shows the modulation characteristics of the DBR lasers. The solid lines show the frequency modulation according to Eq. (16) and the dotted line shows the intensity modulation of the injection current I [14]. Each parameter is defined as follows: $f_r = 10$ GHz and $\Gamma/2\pi = 10$ GHz. $\Gamma_f/(2\pi)^2$ is changed from −80 to 100 (GHz)^2. The direct intensity modulation shows the 3-dB bandwidth of 16 GHz. On the other hand, the frequency modulation exhibits a flat frequency response when $|\Gamma_f|$ is small. Therefore, the frequency modulation is advantageous for the high-speed modulation compared to the intensity modulation. Although f_r is 10 GHz, modulation of over 40 GHz is obtained for frequency modulation. When Γ_f approaches 0, Eq. (16) becomes

$$\frac{M(f)}{M(0)} = 1, \tag{17}$$

where the response does not depend on the modulation frequency. Therefore, Γ_f must be suppressed if we are to achieve both high-speed frequency modulation and high modulation efficiency. In real devices, the operating wavelength should be separated from the bandgap wavelength of

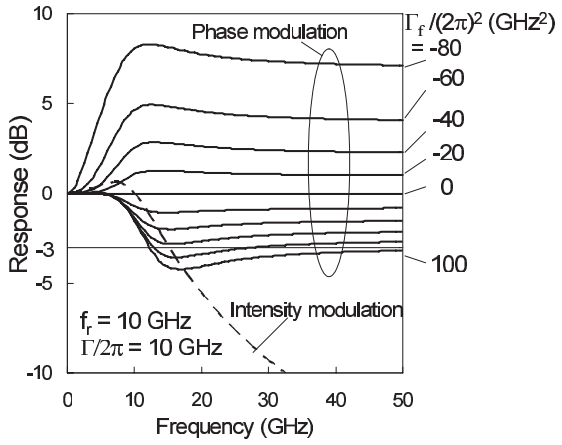

Fig. 3 Modulation characteristics of frequency modulated DBR laser. Solid lines show the phase modulation of the bias voltage in the phase control region and dotted line shows the intensity modulation of the injection current in the active region. The parameter $\Gamma_f/(2\pi)^2$ ranges from −80 to 100 GHz^2 in 20 GHz^2 step. Theoretical parameters are f_r = 10 GHz, $\Gamma/2\pi$ = 10 GHz and $\Delta n_{eq}/n_{eq} = 2.4 \times 10^{-4}$.

the phase control region to avoid any change in the optical loss induced by the quantum confined Stark effect (QCSE) or the Franz-Keldysh effect during reverse bias modulation. Under this condition, the modulation speed is mainly limited by the CR circuit time constant, rather than the relaxation oscillation frequency. Therefore, the phase control region must have a small parasitic capacitance. Since the frequency modulation width is a function of L_p/L, high-efficiency and high-speed modulation is achieved using a short cavity.

2.2 FM/AM Conversion and Transmission

As described in the previous section, a frequency modulated DBR laser makes it possible to generate an ideal high-speed frequency modulated signal. The frequency modulated signal is converted to the intensity modulated signal by using the edge of the optical filter pass-band (FM/AM conversion). In this section, the FM/AM conversion and the transmission property is analyzed theoretically. The time-dependent frequency modulated signal $A_i(t)$ generated from a DBR laser is given by

$$A_i(t) = A_0 \exp(i(2\pi f_0 t + \theta(t))), \tag{18}$$

where A_0 is the signal amplitude, f_0 the lasing frequency, and $\theta(t)$ the phase of the modulated signal. Since the intensity of the signal from the DBR laser is not modulated, A_0 is constant. The modulated lasing frequency is given by

$$f_i(t) = f_0 + \frac{1}{2\pi}\frac{d\theta(t)}{dt}. \tag{19}$$

Using the Fourier transform, the filtered signal $A_o(t)$ is given by

$$A_o(t) = \int T(f)A_i(f)e^{2\pi i f t}df, \tag{20}$$

where $T(f)$ is the filtering function and $A_i(f)$ is the frequency component of $A_i(t)$. The transmitted signal is given

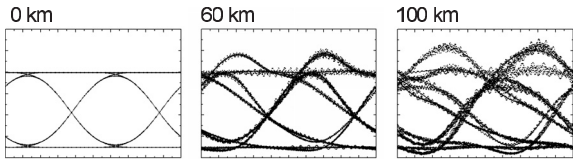

Fig. 4 Simulated eye diagrams after a 10-Gb/s NRZ signal transmission using an MZI filter.

by

$$A_T(t) = \int H(f)T(f)A_i(f)e^{2\pi i f t}df, \tag{21}$$

where $H(f)$ is a transmission function including the dispersion and the transmission loss of the optical fiber.

We simulated the transmission of a 10-Gb/s NRZ signal in accordance with the above procedure. Figure 4 shows the transmission properties calculated by numerical simulation. We employed the Mach-Zehnder interferometer (MZI) filter with a free spectral range (FSR) of 20 GHz for the FM/AM conversion. The lasing frequency for the on state ("1" bit) is set at a frequency 3-GHz lower than the transmission peak frequency of the MZI filter. The optical fiber dispersion is 16.3 ps/nm/km. The frequency modulation width is set at 5 GHz according to the MSK condition. When the MSK condition is applied to the NRZ signal, the phase difference between the "1" values in the "101" sequence becomes π. Under this condition, dispersion induced pulse broadening is effectively suppressed. The MZI filter does not have a reshaping effect on the frequency chirping, however, we observe an open eye diagram after 100-km transmission over non-dispersion shifted fiber by introducing the MSK condition.

3. Demonstration of Transmitters

3.1 Frequency Modulated SSG-DBR Laser

To realize devices based on the theoretical background provided above, we fabricated DBR lasers and demonstrated their transmission characteristics using optical filters. SSG-DBR lasers have excellent wide wavelength tunability using the Vernier effect achieved by injecting current into the DBR regions [15]. We applied this device to widely tunable high-speed transmitters. The fabricated devices are ridge lasers with a multiple-quantum-well (MQW) active layer (8 wells) stacked over a 0.3 μm-thick InGaAsP (λ_g = 1.3 μm) waveguide layer, which is used for the DBR and phase control region. The device structure and fabrication have already been described in detail [11]. The active region is 300 μm long, the phase control region length is 150 μm long, and the front and rear DBR regions are 330 and 620 μm long, respectively. Both facets are anti-reflection coated.

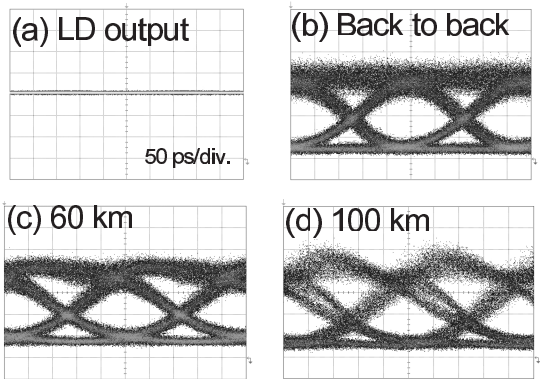

Fig. 5 Measured eye diagrams of a 10-Gb/s NRZ signal using an MZI filter: (a) laser output, (b) filtered signal, and (c) 60- and (d) 100-km transmitted signal.

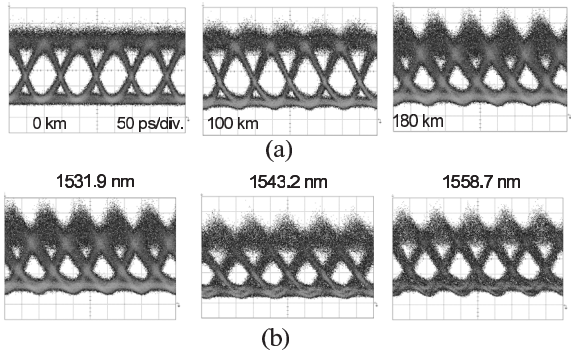

Fig. 6 Measured eye diagrams of a 10-Gb/s NRZ signal using an MZI filter and an etalon filter: (a) transmission characteristics and (b) wavelength tuning characteristics.

3.2 Transmission Characteristics

3.2.1 10-Gb/s Transmission

We demonstrated 10-Gb/s operation and transmission using the fabricated SSG-DBR laser. We employed MZI filter with a FSR of 20 GHz for the FM/AM conversion as calculated in Sect. 2.2. Figure 5 shows measured eye diagrams of 10-Gb/s signals. The lasing wavelength was 1540.6 nm. The bias voltage V_b was −0.5 V, and the modulation voltage V_{pp} was 2.0 V. As seen in Fig. 5(a), little or no intensity modulation was found in the modulated signal from the DBR laser. Figure 5(b) is the signal converted by the MZI filter. Since a clear intensity modulated signal was generated, we can confirm that an ideal frequency modulated signal without intensity modulation is output from the DBR laser. The insertion loss of the Mach-Zehnder filter was 3 dB. Next, we demonstrated the transmission properties. Figure 5(c) and 5(d) are eye diagrams of the transmitted signal. Clear eye openings were obtained after 60- and 100-km transmission. Introduction of the MSK condition leads to increased transmission reach as simulated in Sect. 2.2.

Next, we introduced a combination filter consisting of an MZI filter and an etalon filter with a 3-dB bandwidth of 13.5 GHz. Figure 6(a) shows the transmission characteristics. The lasing wavelength was 1531.9 nm. The bias voltage V_b was −0.54 V, and the modulation voltage V_{pp} was 1.8 V. Clear eye opening was obtained after 180-km transmission with this configuration. The introduction of combination of the filters improves the transmission reach. Figure 6(b) shows the wavelength tuning characteristics. The lasing wavelength was adjusted by injecting current into the front and rear DBRs, and transmission peak frequency of the etalon filter. A tuning wavelength of 27 nm was obtained under the same operating bias and modulation voltage conditions. In this experiment, the tunability was limited by the bandwidth of the erbium-doped fiber amplifier (EDFA) used for the transmission, not the tuning characteristics of the SSG-DBR laser and optical filters. Figure 7 shows the bit error rate (BER) measurement results we obtained for transmission distances of 0 to 180 km. A 9.963-Gb/s NRZ signal with a PRBS of $2^{31} - 1$ was used. V_b was −0.5 V, and the modulation voltage V_{pp} was 2 V. The power penalty for the 180-km transmission at a BER of 10^{-13} was 2.2 dB. The effectiness of implementing the MSK condition and combination of filters was clearly demonstrated.

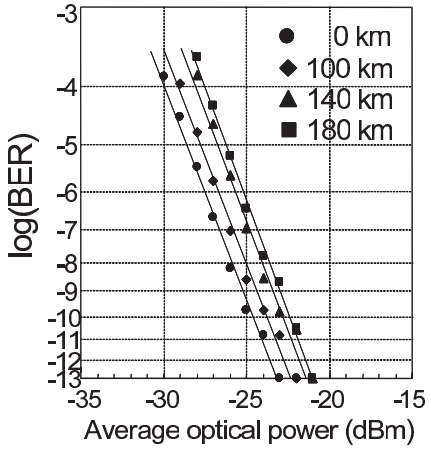

Fig. 7 Bit error rate measurement results for a 10-Gb/s signal transmission using an MZI filter and an etalon filter.

3.2.2 20-Gb/s Transmission

As shown in the Sect. 2.1, the frequency modulated DBR laser makes high-speed operation possible beyond the relaxation oscillation frequency. As a demonstration, 20-Gb/s operation was shown with an SSG-DBR laser. In this experiment, we used a device with a 350-μm long active region and a 200-μm long phase control region length. Figure 8(a) shows the dependence of the eye pattern of the 20-Gb/s operation on the bias current of the active region. V_b was −0.4 V and V_{pp} was 3 V. An MZI filter with an FSR of 40 GHz and an etalon filter were used for the FM/AM conversion. We have also previously measured the relaxation oscillation frequency. The estimated relaxation oscillation frequency changed from 5.3 to 6.8 GHz when the bias

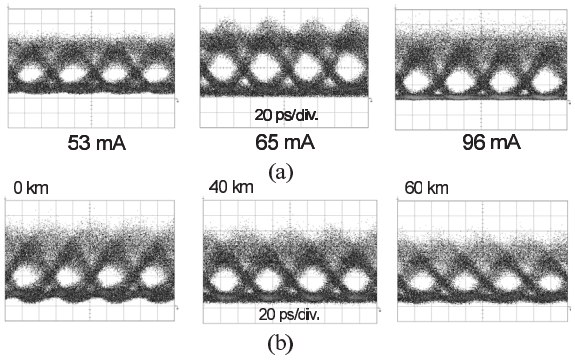

Fig. 8 Measured eye diagrams of a 20-Gb/s NRZ signal using an MZI filter and an etalon filter: (a) dependence on the bias current and (b) transmission characteristics.

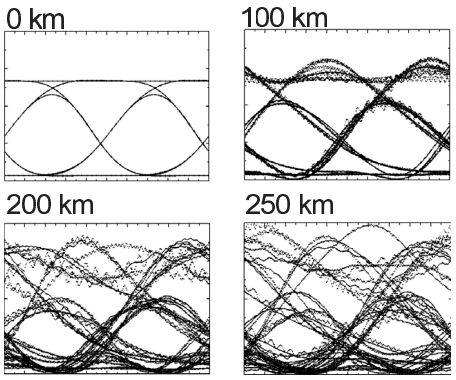

Fig. 9 Simulated eye diagrams of a 10-Gb/s NRZ signal using an MZI and an etalon filter.

current of the active region increased from 53 to 96 mA. The relaxation oscillation frequency is less than 10 GHz, however, the eye diagram was not degraded at any operating bias current. Therefore, we successfully demonstrated high-speed operation independent of the relaxation oscillation frequency.

We investigated the transmission characteristics of a 20-Gb/s signal, and our experimental results are shown in Fig. 8(b). The lasing wavelength was 1538.3 nm, and the operation bias current was 88.7 mA. The bias voltage V_b was −0.9 V, and the modulation voltage V_{pp} was 3 V. Clear eye opening was observed after 60-km transmission.

4. Discussion

As described in Sect. 2.2, the MSK condition allows long-transmission reach. In addition, we have experimentally demonstrated in Sect. 3, that the combination of an MZI and an etalon filter improves transmission reach. Here, we discuss how the use of the reshaping the chirping profile can help enhance the transmission properties. We employed an MZI filter with an FSR of 20 GHz and an etalon filter of 3-dB bandwidth of 13.5 GHz. Figure 9 shows simulated eye diagrams for 10-Gb/s operation. The lasing frequency for the on state is set at a frequency 3-GHz lower than the transmission peak of the MZI and 9.5-GHz lower than the transmission peak of the etalon filter. In addition to the experimental results for the 180-km transmission, a clear eye opening was obtained for transmission of up to 250-km in the simulations. This improvement is enabled by the reshaping of the frequency chirping profile. The principle of reshaping the chirping profile is as follows. The transmission function of the optical filter is approximately given by

$$T(f) = (a + bf + cf^2)\exp(i(d + ef)), \tag{22}$$

where a, b, and c are fitting parameters of the transmittance, and d and e are phase parameters. The lasing frequency after filtering is given by

$$f_o(t) = \frac{1}{2\pi}\frac{d}{dt}\tan^{-1}\left(\frac{\mathrm{Im}(A_o(t))}{\mathrm{Re}(A_o(t))}\right) \tag{23}$$

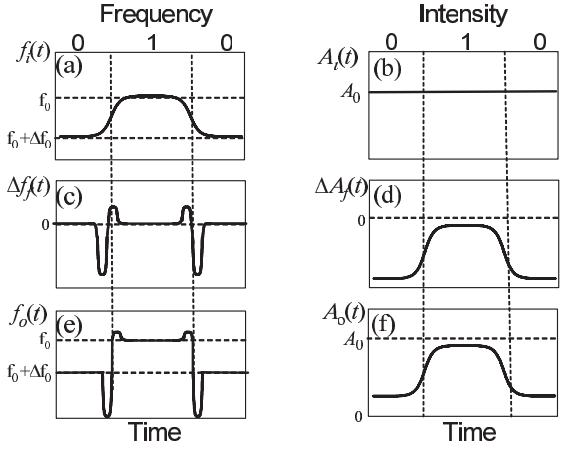

Fig. 10 Schematic of the principle of reshaping the chirping profile using an optical filter. (a) The frequency and (b) intensity profile before filtering, the change of the (c) frequency and (d) intensity after optical filtering, and the (e)frequency and (f) intensity profile after filtering.

$$= f_i(t-e) - \frac{\dfrac{d}{dt}\left(\dfrac{cf_i(t-e)'}{a + bf_i(t-e)' + cf_i(t-e)'^2}\right)}{2\pi\left(1+\left(\dfrac{cf_i(t-e)'}{a + bf_i(t-e)' + cf_i(t-e)'^2}\right)^2\right)} \tag{24}$$

$$\equiv f_i(t-e) + \Delta f_f(t-e). \tag{25}$$

If $c = 0$, there is no chirp reshaping effect since the second term in Eq. (24) vanishes. With the combination of the MZI filter and the etalon filter, $c > 0$ at the operating lasing frequency. Figure 10 is a schematic showing the change in the lasing frequency and amplitude profile of a "010" sequence when the sign of c is positive. Figures 10(a) and (b) show the lasing frequency and intensity of the signal before filtering. Figures 10(c) and (d) show the variation in the lasing frequency and amplitude due to optical filtering. Figures 10(e) and (f) show the signal after filtering. The chirping profile is mainly changed by the second derivative of the lasing frequency f_i''. The effect of reshaping expands the flat chirping region of the "1" bit as shown in Fig. 10(e). In addition, a large dip is inserted in the "0" bits. This dip corresponds to a steep change in the phase. Therefore, if the MSK con-

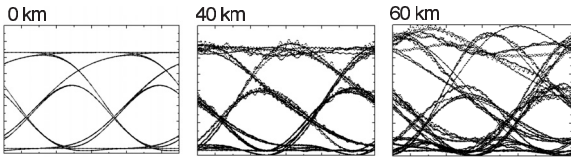

Fig. 11 Simulated eye diagrams of 20-Gb/s NRZ signal using an MZI and an etalon filter.

dition is introduced, the phase modulation condition similar to the duo-binary modulation format is generated since the phase difference between the "1" bits in the "101" sequence is π. Therefore, reshaping the chirping profile extends the transmission performance. On the other hand, if $c < 0$, the flat chirping region narrows (With the MZI filter, $c < 0$).

Next, we investigated the transmission property of a 20-Gb/s signal, and Fig. 11 shows the simulated transmission properties. In the simulations, the frequency modulation width was set at 10 GHz, which is the MSK condition. The lasing frequency for the on state was set at a frequency 4-GHz lower than the transmission peak of the MZI and 4.5-GHz lower than the transmission peak of the etalon filter. Clear eye opening was obtained after 60-km transmission as demonstrated experimentally. The experimental and simulated results show that the introduction of MSK conditions and reshaping the chirping profile are effective in extending the transmission reach.

For practical use, stabilization of the operating wavelength is essential since the lasing wavelength must be locked at the appropriate filtering slope. One possible approach is to use a wavelength locker consisting of etalon filters and power monitoring photodiodes(PDs), as employed in commercial transmitters. The other approach is to use the optical filter for FM/AM conversion as a wavelength locker. If a Mach-Zehnder filter is employed, one port could be used for the signal, and the other port for monitoring. Output power from the monitoring port P_m and the back facet P_b are monitored by PDs. By adjusting the relationship between P_m and P_b with an electrical feedback circuit, the position of the lasing wavelength is locked at the optimum filtering slope.

In addition, high output power from the DBR laser is required because of the filtering loss in the FM/AM conversion. In the case of a transmitter consisting of a DBR laser and a Mach-Zehnder filter for 100-km transmission without an EDFA, 10 dBm of output power will be required if a minimum receiving sensitivity of −20 dBm and the transmission loss of 25 dB is assumed. Since the DBR laser can generate a frequency modulated signal without intensity modulation, the output signal can be effectively amplified by integrating an SOA.

5. Conclusion

In summary, we presented a transmitter using a frequency modulated DBR laser and optical filters. The refractive index modulation of the phase control region with a reverse bias voltage resulted in high-speed frequency modulation. By employing the proposed transmitter, we achieved 180-km error-free transmission of a 10-Gb/s signal with a wavelength tuning range of 27 nm, and clear eye opening after 60-km transmission of a 20-Gb/s signal using SSG-DBR lasers. Also, transmission of a 10-Gb/s signal over 200 km was shown to be feasible in a numerical simulation. We will be able to apply this device to higher bit rate transmission by improving the structure of the DBR laser and the optical filters. A frequency modulated DBR laser has great potential for high-speed, long-reach transmission in future metro and access networks.

Acknowledgments

We thank T. Segawa, Y. Shibata, N. Fujiwara, R. Sato, H. Oohashi, H. Yasaka, H. Suzuki, and R. Takahashi for their technical support and discussions. We also thank K. Ishibashi for fabricating the device, and we thank H. Takeuchi and Y. Tohmori for their encouragement throughout this work.

References

[1] K. Sato, S. Kuwahara, Y. Miyamoto, and N. Shimizu, "40 Gbit/s direct modulation of distributed feedback laser for very-short-reach optical links," Electron. Lett., vol.38, no.15, pp.816–817, July 2002.
[2] M. Radziunas, A. Glitzky, U. Bandelow, M. Wolfrum, U. Troppenz, and J. Kreissl, "Improving the modulation bandwidth in semiconductor lasers by passive feedback," IEEE J. Sel. Top. Quantum. Electron., vol.13, no.1, pp.136–142, Jan./Feb. 2007.
[3] K. Nakahara, T. Tsuchiya, T. Kitatani, K. Shinoda, T. Taniguchi, T. Kikawa, M. Aoki, and M. Mukaikudo, "High extinction ratio operation at 40-Gb/s direct modulation in 1.3-μm InGaAlAs-MQW RWG DFB lasers," Tech. Dig. OFC/NFOEC 2006, no.OWC5, Anaheim, CA, March 2006.
[4] H. Fukano, Y. Akage, Y. Kawaguchi, Y. Suzaki, K. Kishi, T. Yamanaka, Y. Kondo, and H. Yasaka, "Low chirp operation of 40 Gbit/s electroabsorption modulator integrated DFB laser module with low driving voltage," IEEE J. Sel. Top. Quantum Electron., vol.13, no.5, pp.1129–1134, Sept./Oct. 2007.
[5] K. Tsuzuki, Y. Shibata, N. Kikuchi, M. Ishikawa, T. Yasui, H. Ishii, and H. Yasaka, "10-Gbit/s, 200 km duobinary SMF transmission using a full C-band tunable DFB laser array co-packaged with InP Mach-Zehnder modulator," Proc. 2008 International Semiconductor Laser Conference, no.MB6, Sorrento, Italy, Sept. 2008.
[6] P.A. Morton, G.E. Shtengel, L.D. Tzeng, R.D. Yadvish, T. Tanbun-Ek, and R.A. Logan, "38.5 km error free transmission at 10 Gbit/s in standard fibre using a low chirp, spectrally filtered, directly modulated 1.55 μm DFB laser," Electron. Lett., vol.33, no.4, pp.310–311, Feb. 1997.
[7] Y. Matsui, D. Mahgerefteh, X. Zheng, C. Liao, Z.F. Fan, K. McCallion, and P. Tayebati, "Chirp-managed directly modulated laser (CML)," IEEE Photonics Technol. Lett., vol.18, no.2, pp.385–387, Jan. 2006.
[8] D. Mahgerefteh, Y. Matsui, C. Liao, B. Johnson, D. Walker, X. Zheng, Z.F. Fan, K. McCallion, and P. Tayebati, "Error-free 250 km transmission in standard fibre using compact 10 Gbit/s chirp-managed directly modulated lasers (CML) at 1550 nm," Electron. Lett., vol.41, no.9, pp.543–544, April 2005.
[9] K. Iwashita and T. Matsumoto, "Modulation and detection characteristics of optical continuous phase FSK transmission system," J. Lightwave Technol., vol.LT-5, no.5, pp.452–460, April 1987.

[10] T. Sakamoto, T. Kawanishi, and M. Izutsu, "Optical minimum-shift keying with external modulation scheme," Opt. Express, vol.13, no.20, pp.7741–7747, Oct. 2005.
[11] S. Matsuo, T. Kakitsuka, T. Segawa, N. Fujiwara, Y. Shibata, H. Oohashi, H. Yasaka, and H. Suzuki, "Extended transmission reach using optical filtering of frequency-modulated widely tunable SSG-DBR laser," IEEE Photonics Technol. Lett., vol.20, no.4, pp.294–296, Feb. 2008.
[12] S. Matsuo, T. Kakitsuka, T. Segawa, R. Sato, Y. Shibata, R. Takahashi, H. Oohashi, and H. Yasaka, "4 × 25 Gb/s frequency-modulated DBR laser array for 100-GbE 40-km reach application," IEEE Photonics Technol. Lett., vol.20, no.17, pp.1494–1496, Sept. 2008.
[13] J. Langanay, E. Gaumont-Goarin, J.Y. Emery, C. Labourie, J.G. Provost, C. Starck, O. Le Gouezigou, and D. Lesterlin, "High FM bandwidth of DBR laser including butt-jointed electro-optical wavelength tuning sections," Electron. Lett., vol.30, no.4, pp.311–312, Feb. 1994.
[14] G.P. Agrawal and N.K. Dutta, Semiconductor Lasers, Van Nostrand Reinhold, New York, 1993.
[15] H. Ishii, Y. Tohmori, T. Tamamura, and Y. Yoshikuni, "Super structure grating (SSG) for broadly tunable DBR lasers," IEEE Photonics Technol. Lett., vol.4, no.4, pp.393–395, April 1993.

Takaaki Kakitsuka was born in Kumamoto, Japan, in 1971. He received the B.S. and M.S. degrees in physics from Kyushu University, Fukuoka, Japan, in 1994 and 1996, respectively. In 1996, he joined NTT Opto-electronics Laboratories, Nippon Telegraph and Telephone Corporation (NTT), Kanagawa, Japan. He is engaged in research on semiconductor lasers and optical functional devices. He is now with NTT Photonics Laboratories. Mr. Kakitsuka is a member of the Japan Society of Applied Physics and the Physical Society of Japan.

Shinji Matsuo received the B.E. and M.E. degrees in electrical engineering from Hiroshima University, Hiroshima, Japan, in 1986 and 1988, and the Ph.D. degree in electronics and applied physics from Tokyo Institute of Technology, Tokyo, Japan, in 2008. In 1988, he joined NTT Opto-electronics Laboratories, Atsugi, where he was engaged in research on photonic functional devices using MQW-pin modulators and VCSELs. In 1997, he researched optical networks using WDM technologies at NTT Network Innovation Laboratories, Yokosuka. Since 2000, he has been researching high-speed tunable optical filters and lasers for photonic packet switching at NTT Photonics Laboratories, Atsugi. Dr. Matsuo is a member of the IEEE Lasers and Electro-Optics Society (LEOS), Japan Society of Applied Physics.